Temporal Integration Windows in Neural Processing and Perception Aligned to Saccadic Eye Movements

Highlights

- Task, either temporal segregation or integration, was decoded from MEG signals

- Stimulus-evoked activity in occipital cortex alternated at 3 Hz between tasks

- Pre-stimulus, theta-band oscillations were in opposite phase for the two tasks

- Task performance aligned to eye fixations oscillated with opposite theta phase

Authors

Andreas Wutz, Evelyn Muschter, Martijn G. van Koningsbruggen, Nathan Weisz, David Melcher

Correspondence

david.melcher@unitn.it

In Brief

Wutz et al. uncover slow-frequency oscillations between temporal integration and segregation in MEG patterns in visual cortex and in behavioral measures set to eye fixations. The alignment of temporal integration windows to new sensory or oculomotor events may serve as an organizing principle for the temporal processing of continuous sensory input.

CellPress

Current Biology
Article

CellPress

Temporal Integration Windows in Neural Processing and Perception Aligned to Saccadic Eye Movements

Andreas Wutz,[1,2] Evelyn Muschter,[1] Martijn G. van Koningsbruggen,[1,3] Nathan Weisz,[1,4] and David Melcher[1,*]
[1]Center for Mind/Brain Sciences (CIMeC), University of Trento, Rovereto (TN) 38068, Italy
[2]Picower Institute for Learning and Memory, Massachusetts Institute of Technology (MIT), Cambridge, MA 02139, USA
[3]Italian Institute of Technology (IIT), University of Trento, Rovereto (TN) 38068, Italy
[4]Centre for Cognitive Neuroscience, University of Salzburg, Salzburg 5020, Austria
*Correspondence: david.melcher@unitn.it
http://dx.doi.org/10.1016/j.cub.2016.04.070

SUMMARY

When processing dynamic input, the brain balances the opposing needs of temporal integration and sensitivity to change. We hypothesized that the visual system might resolve this challenge by aligning integration windows to the onset of newly arriving sensory samples. In a series of experiments, human participants observed the same sequence of two displays separated by a brief blank delay when performing either an integration or segregation task. First, using magneto-encephalography (MEG), we found a shift in the stimulus-evoked time courses by a 150-ms time window between task signals. After stimulus onset, multivariate pattern analysis (MVPA) decoding of task in occipital-parietal sources remained above chance for almost 1 s, and the task-decoding pattern interacted with task outcome. In the pre-stimulus period, the oscillatory phase in the theta frequency band was informative about both task processing and behavioral outcome for each task separately, suggesting that the post-stimulus effects were caused by a theta-band phase shift. Second, when aligning stimulus presentation to the onset of eye fixations, there was a similar phase shift in behavioral performance according to task demands. In both MEG and behavioral measures, task processing was optimal first for segregation and then integration, with opposite phase in the theta frequency range (3–5 Hz). The best fit to neurophysiological and behavioral data was given by a dampened 3-Hz oscillation from stimulus or eye fixation onset. The alignment of temporal integration windows to input changes found here may serve to actively organize the temporal processing of continuous sensory input.

INTRODUCTION

Despite the presence of constantly changing sensory input, we perceive a continuous and unitary interpretation of the current state of the environment at all times. Perception is faced with opposing system requirements for this real-time processing. Sensitivity to change necessitates high temporal resolution for stimulus segregation, while stability of perceptual representations requires integration of signals over time.

Temporal segregation can occur with millisecond resolution. In humans, flicker-fusion thresholds—the frequency at which intermittent light stimulation appears continuous—range typically between 40 and 60 Hz [1]. Temporal offsets as brief as 5–20 ms can be detected between two sequential stimuli [2, 3], and first-order motion detection can exceed 30 Hz [4]. Neural responses in retinal ganglion cells [5], the lateral geniculate nucleus (LGN) [6], and even in primary visual cortex [7] can track temporal properties driven by fast external stimulation. This high temporal resolution of visual signals supports sensitivity to change and may reduce motion blur ([8, 9]; for a review, see [10]).

Temporal segregation sharply contrasts with the need to integrate information over extended intervals of time to perceive the stability of object identity and location [11, 12], to accumulate information to reach reliable perceptual decisions [13], and to understand sensory signals related to self and object motion [9]. Temporal integration is supported by the brain's capacity for self-organized information retention and is based on persisting neural activity after the input has already vanished [14, 15]. An example of temporal integration is the finding that two flashes separated by a brief delay may be perceived as a single item when the inter-stimulus blank period is less than ∼50 ms [16]. Similarly, in forward- and backward-masking paradigms, integration of target and mask is reported for delays of 80 to 120 ms [17]. Another example of integration is the perception of apparent motion between two briefly flashed stimuli, which can occur across a temporal gap of hundreds of milliseconds [e.g., 18].

Here, we aim to characterize the neural mechanisms that determine whether two stimuli are temporally integrated into a single event or, instead, perceived as separate entities. To this end, we directly contrast the time course of stimulus segregation and integration with a variant of the missing-element task [19, 20]. Human observers viewed the same sequence of two patterns separated by a brief inter-stimulus interval (ISI) but were instructed to either segregate or integrate stimuli over time (Figure 1A). On integration trials, participants were instructed to report the location of the missing element, which was the single cell in a virtual grid where no item was presented in either the first or the second display. This task was only possible when the two
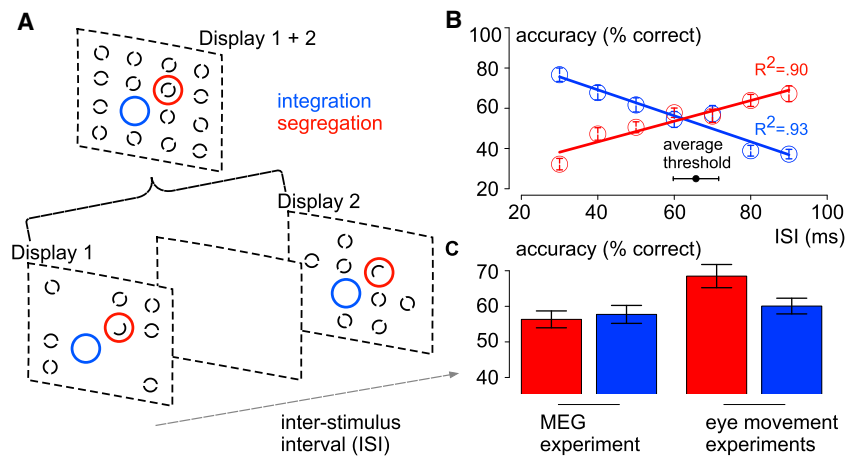
Figure 1. Experimental Stimuli and Behavioral Data

(A) Variant of the missing-element paradigm [14] measuring perceptual integration and segregation of stimuli over time. A blank inter-stimulus interval (ISI) separates the two stimulus frames, and participants are instructed to locate either the missing element (which requires temporal integration) or the odd element (segregation) in separate blocks.

(B) Linear fits on mean integration and segregation performance (circles; ±1 SEM) [21] as a function of ISI. Task thresholds are calculated for each subject (N = 19) as the between-task intersection point of the inversely linear functions over ISI.

(C) Mean task performance (±1 SEM) [21] with constant ISI over the course of the experiments (MEG: n = 19; eye movement: n = 28).

displays were combined over time [19, 20]. On segregation trials, in contrast, the task was to report the location in which an odd element (half annulus) was shown in both displays. Performance in the latter task required the two displays to be segregated in time, since integration of the two half annuli rendered them indistinguishable from a full annulus. As expected, performance was near perfect for the integration task with a brief ISI and worsened with longer delays [19, 20], while segregation showed the opposite pattern (Figure 1B). For each subject, we determined the ISI at which performance on the two tasks was matched; yielding equal proportions between correct/incorrect trials for both segregation and integration tasks (Figure 1C). Thus, this stimulus display allowed us to match task difficulty and to use the identical physical stimulus while measuring the brain mechanisms underlying temporally separate or combined visual percepts.

We tested the hypothesis that the visual system coordinates stimulus segregation and integration over time by aligning the phase of slow-frequency brain oscillations to the onset of newly arriving sensory samples. First, we used magneto-encephalography (MEG) to compare the converging measures of stimulus-evoked fields, frequency-specific phase coherence, and multivariate pattern analysis (MVPA) decoding between segregation and integration trials. Across all three MEG measures, we found a task-specific pattern of brain states for either segregation or integration in alternation at 3 Hz after stimulus onset, possibly due to a phase shift in ongoing brain oscillations. Consistent with our hypothesis, oscillatory activity in the pre-stimulus time interval was already informative about both task processing and behavioral outcome, with opposite phases in the theta frequency band for segregation/integration, as well as distinguishing correct/incorrect trials for each task separately.

In a second study, we investigated the role of saccadic eye movements in shifting slow-frequency alternations between task states. Like stimulus onset, each saccade confronts the visual system with a transient change in sensory input, creating a conflict between stimulus segregation and integration. Analogous to the temporal patterns decoded from the MEG data when aligned to stimulus onset, the densely sampled time courses of task performance alternated at a rate of 3–5 Hz when aligned to the onset of each new eye fixation. Together, these findings uncovered a counter-phase alternation between

pattern segregation and integration in visual processing that determined perceptual experience.

RESULTS

Psychophysics

The ISI that yielded equal proportions of correct trials for both tasks was determined individually for each subject prior to running the MEG experiment (Figure 1B; see Supplemental Information). Integration performance decreased, and segregation increased with longer ISI, with ISI explaining more than 90% of the variance (Figure 1B). The average threshold over subjects was 68 ± 27 ms. In behavioral experiments, the ISI was fixed at 50 ms. For both experiments, performance did not differ significantly between tasks: MEG experiment, t(18) = −0.4, n.s. (not significant); eye movement experiment, t(27) = 1.8, n.s.) (Figure 1C).

MEG Data

The analysis of MEG data focused on differences in neural activity, for an identical stimulus and with matched task difficulty, as a function of task (integration/segregation) and performance (correct/incorrect). This involved the analysis of event-related fields (ERFs), inter-trial phase coherence (ITC), and MVPA decoding in the post-stimulus time period, plus theta frequency band phase bifurcation in the pre-stimulus period.

Stimulus-Evoked Activity: ERF and ITC

First, we investigated stimulus-evoked activity in the time interval ranging from the second stimulus display onset to +500 ms afterward, as measured by the ERF and ITC (see Supplemental Information). Statistical significance between conditions was assessed by means of nonparametric cluster-based permutation t statistics, effectively controlling for multiple statistical comparisons at multiple time, frequency, and sensor samples (see Supplemental Information). Both measures (ERF and ITC averaged over frequencies between 5 and 25 Hz) resulted in strong response peaks relative to pre-stimulus baseline periods: z(ERF) = 2.5, and z(ITC) = 2.3. As shown in Figure 2, the relative strength of the evoked activity alternated between tasks, time locked to stimulus onset. For the ERF, segregation trials evoked a stronger response from 160 to 290 ms after display 2 onset
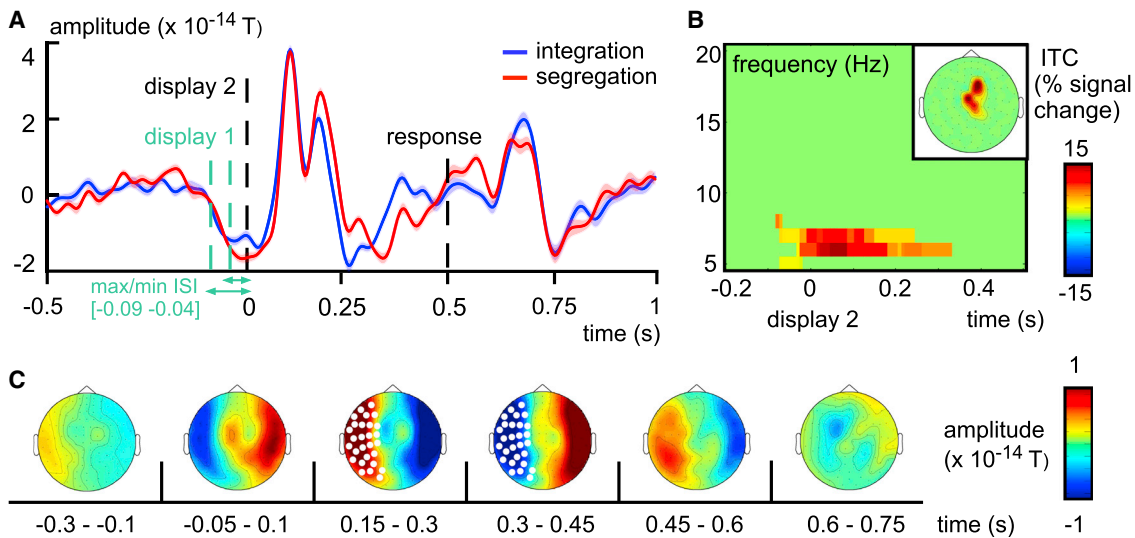
Figure 2. MEG-Stimulus Evoked Activity

(A) Grand-average ERF (n = 19) time locked to the onset of the second stimulus display and averaged over a significant left temporal magnetometer sensor cluster (see white dots in C). Shaded areas reflect ±1 SEM [21].

(B) Signal change in ITC, (segregation − integration)/integration, averaged over a significant central gradiometer sensor cluster (see top inset). Non-significant effects (p < 0.05) are masked.

(C) Difference in topographies (segregation − integration) averaged over successive 150-ms intervals from pre- to post-stimulus periods.

(cluster-corrected p < 0.004). Then, the pattern reversed so that the same sensor locations displayed stronger evoked amplitude in integration trials from 300 to 450 ms (cluster-corrected p < 0.007; Figure 2A). Averaged over this significant cluster of sensors (highlighted with white dots in Figure 2C), evoked activity alternated four times between segregation and integration trials in time windows of approximately 150 ms in duration, starting from the onset of the stimulus sequence until +600 ms (Figure 2C): −250 to −100 ms, t(18) = 1.9, n.s.; −50 to +100 ms, t(18) = −3.7, p < 0.002; +150 to 300, t(18) = 5.3, p < 0.001; +300 to +450, t(18) = −6.2, p < 0.001; +450 to +600 ms, t(18) = 2.5, p < 0.024; +600 to +750 ms, t(18) = −0.5, n.s.). This ERF effect could result either from differences in stimulus-evoked response amplitude or stimulus-reset phase coherence between conditions. In order to disentangle these possibilities, we estimated the amount of phase alignment to stimulus onset with ITC. Both ERF and ITC activity peaked around 100 ms after display 2 onset (mean ± SD: 120 ± 56 ms for ERF, and 98 ± 31 ms for ITC; no latency difference, t(18) = 1.6, n.s.), and the baseline-corrected effect sizes correlated moderately over subjects (r = 0.41, p < 0.085). Between tasks, we found a stronger ITC for segregation trials immediately after display 2 onset (0 to +150 ms) at 6–7 Hz within a central gradiometer sensor cluster (Figure 2B; cluster-corrected p < 0.001 for the time interval from −200 to +500 ms and the frequency range between 5 and 25 Hz). Confirming previous results using integration masking [22], these findings suggest that the initial stronger response for segregation trials, evident in the ERF, was, at least in part, due to stronger phase coherence of slow-frequency oscillations.

Multivariate Analysis: MVPA

We used MVPA classification to further investigate the differences in the post-stimulus time period as a function of task (integration/segregation) and behavioral outcome (correct/incorrect; see

Supplemental Information). Task was decodable as early as 100 ms after the second stimulus display onset (cluster-corrected z_{cor} = 3.1, p < 0.002), peaked at 260 ms (z_{cor} = 3.7, p < 0.001), and persisted for almost an entire second (z_{cor} = 3.2, p < 0.002 at 950 ms; Figures 3A and 3B). Across subjects, the highest decoding accuracy (z(task decoding) = 2.3; measure and baseline intervals identical to those mentioned earlier) correlated significantly with ERF (r = 0.55, p < 0.015) and ITC effect sizes (r = 0.59, p < 0.008) but peaked in a significantly later time interval (mean ± SD: 353 ± 96 ms; decoding versus ERF peak latency, t(18) = −9, p < 0.001; versus ITC, t(18) = −12.2, p < 0.001). Topographical maps and source projections (see Supplemental Information) revealed two temporally distinct time windows (150–450 ms and 600–900 ms), with maximal decoding accuracy at occipital-parietal sensor locations and occipital-parietal sources (Figure 3C; Table S1).

The MEG signal also contained information about task outcome in terms of correct or incorrect trials, separately for integration or segregation blocks. For segregation, we found significant above-chance decoding of outcome by 140 ms after display 2 onset (z_{cor} = 2.1, p < 0.037). However, outcome decoding was most accurate and reliable in the time window from around +500 to +900 ms, when the participants' response was probed (Figures 3A and 3B; see also Figure 2A) (for segregation: peak sample at 570 ms, z_{cor} = 3.7, p < 0.001; for integration: peak sample at 620 ms, z_{cor} = 2.3, p < 0.022). For both integration and segregation blocks, the lcmv beamformer algorithm (see Supplemental Information) suggested neural generators in occipital areas as source solutions for outcome decoding, indicating that the MVPA signal reflected perceptual rather than purely decisional or motor processes (Figures 3D and 3E; Table S1). Statistical significance was assessed by means of cluster-corrected z statistics of decoding accuracy against chance
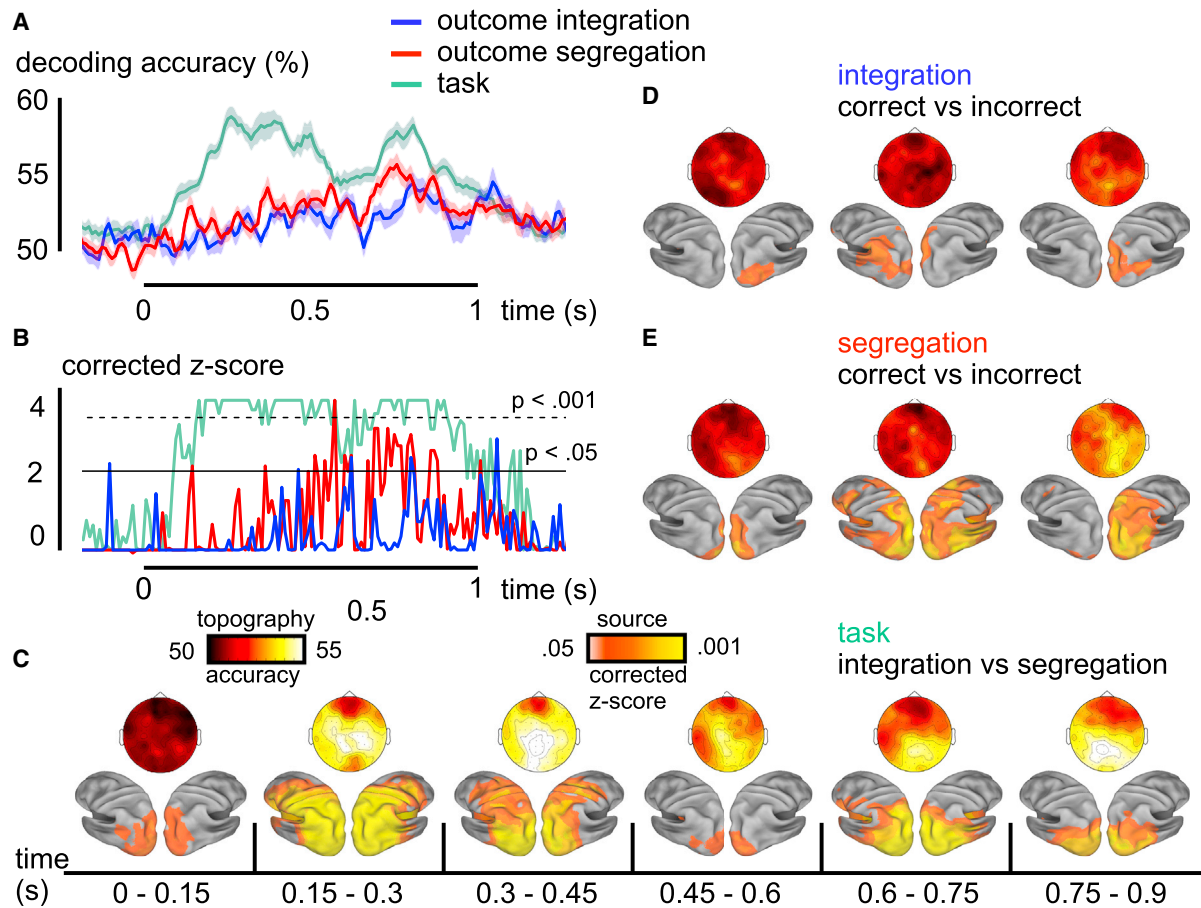
Figure 3. MEG-MVPA Decoding

(A) Mean MVPA decoding accuracy for task and outcome. Shaded areas reflect ±1 SEM [21].

(B) Cluster-corrected z scores for task and outcome.

(C–E) Sensor topographies and neural sources for MVPA decoding of task (C) and outcome (D for integration, E for segregation).

See also Figures S1 and S2 and Table S1.

level, using a threshold-free method for clustering and a Monte Carlo permutation approach for multiple comparison correction (see Supplemental Information). MEG-MVPA decoding was equally robust when the sensor topographies were normalized for overall response amplitude (Figure S1) and/or when chance level was estimated based on random permutations of the data partitions (in contrast to assuming chance level as 50% a priori; Figure S2).

The temporal generalization method (see Supplemental Information) was used to characterize the temporal pattern of task decoding and its interaction with task outcome (correct versus incorrect). As shown in Figure 4A, we generated matrices mapping each classifier's task-decoding accuracy in the training set against the entire testing time interval from −500 to +1,500 ms, relative to display 2 onset (in steps of 10 ms). The strong above-chance decoding accuracy along the main diagonal suggests a series of distinct patterns of brain activity for integration versus segregation trials (z_{cor} = 3.3, p < 0.001; training/testing time, +280/270 ms). On-diagonal, above-chance decoding was accompanied by off-diagonal, below-chance accuracy, with consistent and highly significant misclassification of

integration and segregation trials during the earlier and later intervals (around 150–300 ms before and after) on the basis of the trained pattern at a given time point (z_{cor} = −3.3, p < 0.001; training/testing time, +780/500 ms; Figure 4A). This pattern suggests that the signal dissociating task processing reoccurred at a later time point, but with reversed polarity. The pattern of reversed decoding persisted for almost an entire second after stimulus onset (Figures 4A and S3; Table S2), originated in occipital brain regions for both the on- and the off-diagonal signals (Figure 4B; Table S1), and alternated at a rate of approximately 3 Hz (Figures 4C and 4D). The strength of task decoding (segregation versus integration trials) interacted with task outcome. Decoding was significantly better in correct trials (used in both training and testing sets), with more accurate classification for the on-diagonal signal and stronger misclassification for the off-diagonal signal (Figures 4C and S4; Tables S3 and S4). In other words, incorrect segregation/integration trials were more likely to be classified as belonging to the other task, respectively. This resulted in significantly stronger 3-Hz amplitude in decoding accuracy for correct trials (3.3-Hz amplitude peak, correct versus incorrect, t(18) = 3.2, p < 0.006; Figure 4D).
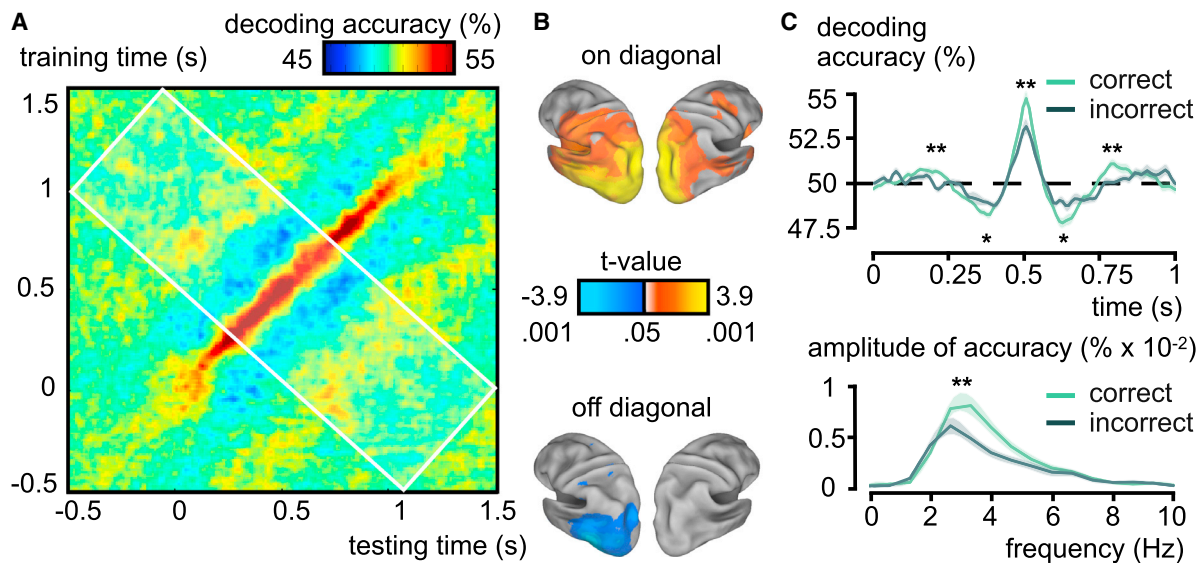
Figure 4. Generalization over Time and Outcome of the Task-Decoding MVPA Signal

(A) Temporal generalization matrix of mean task decoding accuracy (segregation versus integration; n = 19).

(B) Neural sources for on-diagonal (testing time: 475 ± 25 ms) and off-diagonal (testing time: 725 ± 25 ms) decoding signals based on training time classifiers of 475 ± 25 ms.

(C) Top: time course of mean task decoding accuracy along the anti-diagonal (±250 ms; white shaded rectangle shown in A) separately for correct and incorrect trials. Bottom: the spectral amplitude of the Hanning-tapered and demeaned time courses.

Asterisks indicate decreasing p values (*p < 0.05; **p < 0.01; ***p < 0.001) for correct versus incorrect trials. Shaded areas reflect ±1 SEM [21]. See also Figures S3–S5 and Tables S1–S4.

Consistent with univariate analysis, MVPA temporal generalization confirmed that task processing alternated at a rate of approximately 3 Hz. However, the most prominent pattern between segregation and integration signals was the robust phase opposition in the first two 150-ms time windows after the stimulus-evoked response. Additionally, we found indications for further alternations but with decaying signal amplitude from the time-locking event (Figures 2A, 2C, 4C, and 4D). In order to estimate the longevity of the task-dissociating pattern and how often the signal alternated between segregation and integration states, we compared the explained variance (least-square) in the task-decoding signal between the best-fitting models from three different model classes: oscillatory (sinusoid function, or S), decaying (Gabor function, or D) or dampened oscillatory (Sinusoid Function × Decay Function, or DS; see Supplemental Information).

The best-fitting dampened sinusoid function provided a strong explanation for the observed mean decoding signal ($R^2 = 0.89$; Figure S5), accounting for significantly more variance compared to the optimal sinusoid function ($R^2 = 0.31$) or monotonic response decay function ($R^2 = 0.61$; change in R^2 – F test: DS versus S, $F(1, 147) = 781.7$, $p < 0.001$; DS versus D, $F(2, 147) = 185.9$, $p < 0.001$). Averaged across the single-subject parameter estimates, both steady and dampened sinusoid functions were best fit with a signal alternation rate around 3 Hz (mean frequency ± SD [f]: for S, f = 2.9 ± 0.5 Hz; and for DS, f = 3.4 ± 0.4 Hz). In contrast to a longer-lasting ongoing alternation between tasks, however, the dampened oscillation model accounted for the signal variance foremost in a limited time window of one or two cycles from stimulus onset (mean ± SD for full-duration half maximum [FDHM] = 395 ± 224 ms, 1.3 ± 0.5 cycles).

Pre-stimulus Oscillatory Activity

The dampened oscillatory pattern might be evident of a phase reset in ongoing brain oscillations [23, 24], aligning the optimal phases for segregation and integration to the onset of the stimulus display. In order to directly test whether a shift in oscillatory phase accounted for the alternations between task signals observed here, we analyzed the oscillatory activity in the pre-stimulus period. If the observed, stimulus-evoked alternations were due to a phase shift in ongoing oscillations, the phase information of slow-frequency oscillations before stimulus onset should be informative about task processing and/or behavioral outcome. To this end, we first extracted the instantaneous phase in the theta frequency band (3- to7-Hz band-pass-filtered time courses; Figure 5A) for the 1-s time period preceding the onset of stimulus display 1 with a Hilbert transform. Then, we calculated the phase bifurcation index (PBI) [25] between segregation and integration trials, as well as between correct and incorrect trials for each task separately. Statistical significance was assessed with a permutation approach based on 10,000 surrogate datasets with shuffled condition labels and corrected for multiple comparisons with the false discovery rate procedure (see Supplemental Information). A positive PBI indicates that two conditions exhibit strong phase coherence (as measured with ITC) but at polar-opposite phase angles: PBI = (ITC_{cond1} − $ITC_{all\ trials}$) × (ITC_{cond2} − $ITC_{all\ trials}$; see Supplemental Information). Consistent with our hypothesis, we found significant phase bifurcation in the pre-stimulus interval between segregation and integration trials (smallest p < 0.01), mainly over occipital sensor
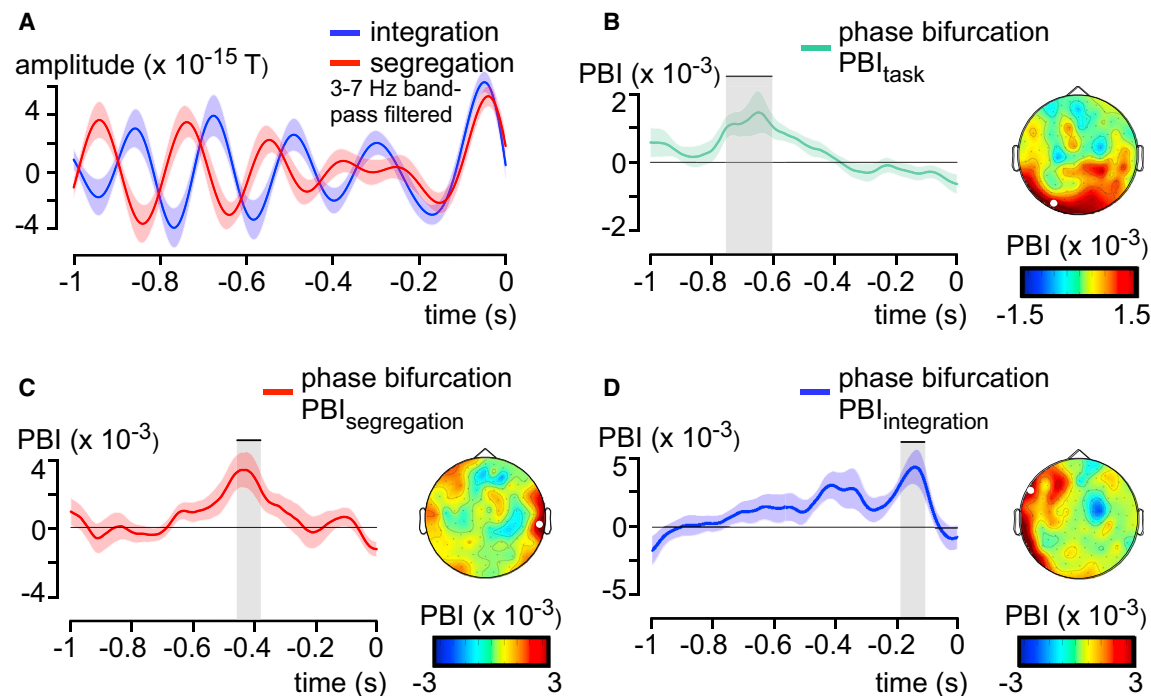
Figure 5. Theta Phase in the Pre-stimulus Time Window

(A) Grand average (n = 19), theta-band-pass-filtered (3–7 Hz) time series in the pre-stimulus interval for the sensor with maximal phase bifurcation (see white dot on topography in B).

(B) Left inset: phase bifurcation index (PBI) for task in the pre-stimulus interval for the same sensor: $PBI_{task} = (ITC_{segregation} - ITC_{all}) \times (ITC_{integration} - ITC_{all})$. Significant time points are shaded in gray. Right inset: corresponding sensor topography averaged over significant time points. The white dot highlights the sensor with maximal PBI.

(C and D) Pre-stimulus phase bifurcation and corresponding topographies for outcome: $PBI_{outcome} = (ITC_{correct} - ITC_{all}) \times (ITC_{incorrect} - ITC_{all})$ (C for segregation, D: for integration). Shaded areas reflect ±1 SEM [21].

See also Figure S6.

locations (19/102 significant magnetometer sensors, p < 0.05; Figure 5B). In addition, for each task separately, we observed significantly stronger phase opposition than expected by chance between correct and incorrect trials over temporal sensor locations (for integration: smallest p < 0.023, ten significant sensors; for segregation: smallest p < 0.021, six significant sensors; Figures 5C and 5D). We found positive phase bifurcation indicative of phase opposition between tasks, mainly in the pre-stimulus time window. After stimulus onset, phase coherence (ITC) was stronger in segregation trials (as also shown in the stronger ITC effect reported earlier), which resulted in a negative PBI for task processing due to stronger phase locking to stimulus onset in one condition (Figure S6).

Behavioral Data Aligned to Eye Movements

Next, we tested whether this pattern of alternations between temporal integration and segregation in the theta frequency band has perceptual consequences. In the MEG study, we predicted that stimulus onset would lead to a phase reset of ongoing slow-frequency oscillations, and we were able to trace the effects of the onset on neural signals at subsequent points in time. For behavioral oscillations, however, it is necessary to define a reset point prior to the stimulus/probe in order to trace the time course of performance aligned to that event [26–29].

We hypothesized, based on both theoretical reasons [30, 31] and neurophysiological evidence for theta-band phase resets after saccades [32–36], that fluctuations would be aligned to new fixations. Moreover, it has been shown that phase alignment influences the temporal precision of neural coding [32, 37], leading to the hypothesis that segregation performance, which relies on high temporal precision, might be best after a saccade-induced reset.

On each trial, we measured the onset of an 8° saccadic eye movement and then timed stimulus presentation relative to eye fixation onset. Stimuli were presented over the first 500 ms (20-ms time bins, 50-Hz sampling) in experiment 2A (Expt 2A) or the entire first second after eye-fixation onset in experiment 2B (Expt 2B) (40-ms bins, 25 Hz; Figure 6A). Subsequently, we calculated the proportion of correct responses at each time point (dense sampling [26]; see Supplemental Information). We hypothesized that the saccade, like the stimulus onset in the MEG study, would create a phase reset and lead to alternations in performance, with an initial benefit for segregation trials.

Consistent with this hypothesis, the temporal dynamics for segregation and integration differed significantly with alternations between the two tasks in terms of accuracy occurring in 150-ms time windows for both Expts 2A and 2B (Figure 6B; Tables S5 and S6). Following the logic used in previous studies
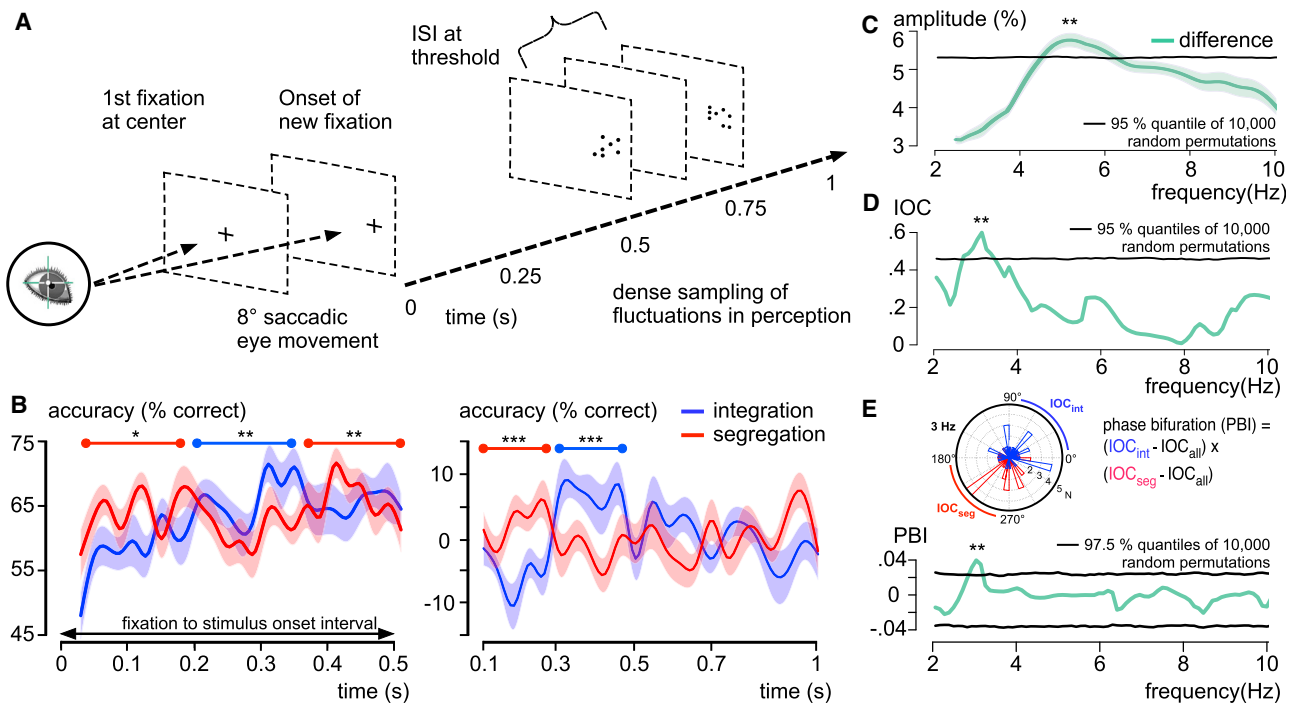
Figure 6. Paradigm and Results for Eye-Movement-Aligned Behavioral Performance

(A) Experimental paradigm for measuring the time course of integration and segregation time locked to eye fixation onset.

(B) Time course of mean task performance as a function of fixation-to-stimulus onset interval (left panel: raw accuracy in Expt 2A; middle panel: linear detrended accuracy in Expt 2B; both ns = 14). Asterisks indicate decreasing p values (*p < 0.05; **p < 0.01; ***p < 0.001) for segregation versus integration. Shaded areas reflect ±1 SEM [21].

(C) Mean amplitude spectrum for the difference time course (segregation − integration) in Expt 2B. Shaded areas reflect ±1 SEM [21].

(D) Inter-observer phase coherence (IOC) of the difference time course in Expt 2B.

(E) Upper panel: phase angle distribution at 3 Hz for integration and segregation time courses across subjects (data from all subjects in Expts 2A and 2B; n = 28). Lower panel: phase bifurcation index (PBI) for the raw time courses in Expt 2B.

Asterisks in (C)–(E) indicate decreasing p values (*p < 0.05; **p < 0.01; ***p < 0.001) for empirical versus random data. See also Figure S5 and Tables S5 and S6.

measuring behavioral oscillations [26–29], we Fourier-transformed the accuracy time courses for each task and the difference time course between tasks (segregation-integration) in order to reveal temporal structure in data. Statistical reliability of the peaks in the Fourier spectra was assessed with a nonparametric permutation approach based on shuffled surrogate data.

The spectral amplitude of the accuracy-difference time course between tasks revealed a significant peak at 5.2 Hz (Expt 2B: permutation test, p < 0.009; Figure 6C). Likewise, the phase of the complex Fourier vectors across observers at 3 Hz deviated significantly from a uniform distribution (Rayleigh test: Expt 2A, 3.75 Hz, z = 4.2, p < 0.0125; Expt 2B, 3.1 Hz, z = 5, p < 0.005) and was significantly more concentrated (inter-observer coherence [IOC]; see Supplemental Information) compared to random time series (permutation test: Expt 2A, p < 0.015; Expt 2B, p < 0.004; Figure 6D). To confirm the phase opposition between the two tasks, we assessed the average angular phase relation across observers between integration and segregation with the PBI that is sensitive to strong phase locking across observers (IOC) at polar-opposite angles ([25]; see Supplemental Information). A counter-phase relationship indicative of a phase shift between integration and segregation time series was found at 3 Hz in both experiments (permutation test: Expt 2A, 3.3 Hz, p < 0.004; Expt 2B, 3 Hz, p < 0.009; Figure 6E). Taken together,

the time course, spectral amplitude, and spectral phase analyses indicate that integration and segregation performance alternated in the theta range (≈3–5 Hz) and in counter-phase locked to the new eye-fixation onset.

Similar to the modeling approach for the MEG data, we estimated the longevity of these behavioral oscillations with least-square curve fitting of the accuracy-difference time course with a sinusoid function (or S), a decaying function (or D [exponential]) or a combination of the two (DS). The average behavioral time course in Expt 2A (+110 to +510 ms) was equally well modeled by a sinusoid function (f = 3.6 Hz, R^2 = 0.49) or damped-ened sinusoid function (f = 3.5 Hz; half-life [$t_{(1/2)}$] = 401 ms (1.4 cycles), R^2 = 0.47), both explaining significantly more variance compared to a monotonic decay (R^2 = 0.22; F test: S versus D, $F_{(1, 18)}$ = 7.8, p < 0.012; DS versus D, $F_{(2, 18)}$ = 4.2, p < 0.033). For Expt 2B, the behavioral time course (+160 to +1,000 ms) was best fit with a dampened sinusoid function (f = 2.9 Hz, $t_{1/2}$ = 143 ms [0.4 cycles], R^2 = 0.57; Figure S5), followed by a steady sinusoid function (f = 2.9 Hz, R^2 = 0.33), and then a decaying function (R^2 = 0.22; F test: DS versus S, $F_{(1, 19)}$ = 9.3, p < 0.007; DS versus D, $F_{(2, 19)}$ = 6.8, p < 0.006; S versus D, $F_{(1, 19)}$ = 4.3, p < 0.051). Thus, in accordance with the MEG results reported earlier in the text, the behavioral oscillations between integration and segregation decayed with

CellPress

increasing time from fixation onset, evident of short-lived phase synchronization triggered by the saccadic eye movement.

DISCUSSION

The findings reported here uncover the temporal coordination of opposing processing demands for segregation and integration. For MEG, we found an alternating temporal pattern between segregation and integration in converging ERF, ITC, and MVPA measures, as well as pre-stimulus phase. MEG-MVPA task decoding correlated highly with classical measures of visual evoked activity (ERF, ITC) and spread over time in the caudal-to-rostral direction. Consistent with previous studies using electroencephalography [38], we found the strongest MEG signatures of pattern integration/segregation in intervals after the first feed-forward sweep of visually evoked activity (~150–450 ms). Critically, neither peak intensity nor latency of any MEG measures (ERF, ITC, MVPA) was correlated with the temporal offsets between the two stimulus frames for individual observers (r < 0.35, all ps were n.s.). Hence, the latency in evoked activity between segregation and integration time courses does not simply reflect a short-lived effect of selecting different target displays, i.e., selection of the first or second display for segregation or integration, respectively. MVPA generalization showed that integration and segregation trials were predominantly decoded from the MEG signal on the basis of a pattern that reverses polarity with a period of approximately 150 ms, consistent with a dampened 3-Hz oscillation alternating for a limited time window of one or two cycles. Importantly, the MVPA decoding pattern between tasks (segregation versus integration) interacted with task outcome, consistent with its holding functional relevance for perception. To the best of our knowledge, this provides the first report of significant MVPA decoding of top-down signals (i.e., task instructions) in visual cortex using MEG, with decoding performance in line with recent reports decoding top-down factors using functional magnetic resonance imaging (fMRI) [39].

In the MEG study, we measured alternations in segregation/integration time locked to stimulus onset. Time-frequency analysis of the pre-stimulus time period suggested that the post-stimulus neural signals were due to a phase shift in ongoing brain oscillations favoring either task in opposite phases in the theta frequency band.

In natural viewing, however, it is more typically the case that the stimulus is continuously present but discretely sampled by saccadic eye movements at a rate of about 3–5 Hz [15]. In the second experiment, we show that the visual system aligns its susceptibility for segregation and integration to this overt sampling behavior. When time locked to fixation onset, behavioral performance alternated in time in the theta frequency range, with a phase alignment similar to that of the stimulus-locked MEG activity.

Interestingly, performance, when time locked to either stimulus onset or fixation onset, was initially better for segregation. One possible explanation is that performance in the segregation task relies on high temporal resolution. In terms of neural processing, high temporal resolution may reflect precision in spiking activity; for a review, see [37]. Such increases in spike rate precision have been linked to both ongoing and saccade-induced

oscillations [32, 37]. For perception, high temporal resolution may be critical for encoding dynamic stimuli as well as supporting rapid scene segmentation [40]. In the case of saccades, the bias toward segregation may also reflect the need of the visual system to preserve separate retinal images across saccades or may be a strategy to account for lingering effects of saccadic remapping [30, 41].

Because eye movements are used to actively sample the environment, the close coordination between motor and sensory systems found here might compensate for the drastic sensory changes associated with each saccade and prepare the visual system for a new spatiotemporal pattern of input with each new fixation; for reviews, see [30, 31, 41]. Consistent with this idea, recent neurophysiological studies have demonstrated saccade-related phase resets of ongoing oscillations in the local field potential of temporal lobe regions during natural viewing [32–34] and, in particular, in theta frequencies around 3–5 Hz [35, 36]. Here, we show that saccades reset fluctuations in human perceptual processing consistent with a dampened oscillation in the theta range (3–5 Hz). The alignment of processing to new fixations, either by resetting ongoing oscillations or by creating a new fluctuation ex novo, influenced processing for less than 1 s, possibly due to factors such as the intentions to make further saccades or micro-saccades (resetting the fluctuation) or neural oscillators moving out of phase.

For both MEG and behavioral measures, integration performance became more dominant in the second phase. Integration supports the more extended processing of dynamic or complex stimuli [42] and may ensure the consolidation and stability of specific object representations over time and across saccades [11, 12, 18, 30]. However, integration requires temporal buffering of sensory input for extended processing, at the cost of temporal precision and local details [37]. Thus, there is a natural trade-off between the needs for integration and segregation.

One potential explanation for the overall pattern of results found here is that perceptual outcome, in terms of whether two stimuli are integrated or segregated, may depend on a single oscillatory mechanism [16, 22, 43–45]. For example, studies of trial-by-trial variability in seeing two flashes as either a single event or two events [16, 45], as well as studies of integration masking [22], have also shown that the ability to segregate two stimuli depends on the timing of those events with respect to the phase of oscillatory activity. This finding has been interpreted as evidence for a "serial," bottom-up mechanism in which perception is determined by whether the two stimuli fall into the same, or different, cycles [16]; see also [46]. Such studies, which used variants of a temporal segregation task, rather than both integration and segregation, suggest that cortical oscillations provide natural temporal frames for the grouping or chunking of neural activity [43, 44].

Alternatively, sensory systems might perform integration and segregation, at least partially, in parallel, and the time course differences found here might, then, result from an active, top-down bias toward either state. Information initially used to segregate the two displays (in the first phase) may be maintained in a temporal buffer/window in order to also support temporal integration in the second phase, followed by segregation again in the third phase. Previous trans-cranial magnetic stimulation (TMS)

studies have demonstrated such long-lasting biasing signals for feature integration in visual cortex [47]. In addition, evidence for retention of information across multiple oscillatory cycles comes from studies showing regularly recurring ''perceptual echoes'' at 10 Hz [48] and integration cycles at 5 Hz for repeated natural images [49].

In conclusion, the present study provides converging evidence for behavioral and neural oscillations in states of neural susceptibility and suggests that these alternations may play a role not just in the detection of sub-threshold stimuli [25] but also, more generally, in the parsing of continuous sensory input. Specifically, these findings link alternations in neural processing and perception to phase reset/alignment based on input transitions such as stimulus onsets or saccadic eye movements. Overall, these findings suggest that the alignment of integration windows to new sensory or oculomotor events may serve as an organizing principle for the temporal processing of continuous sensory input.

EXPERIMENTAL PROCEDURES

All procedures were approved by the ethics committee of the University of Trento. Participants gave written, informed consent before each experimental session. In all experiments, participants viewed the same sequence of two patterns separated by a brief ISI but were instructed to locate either the missing element (which requires temporal integration) or the odd element (segregation) in separate blocks (Figure 1A). We used a blocked design based on pilot studies, which showed that participants were worse at performing both tasks simultaneously. In a random-trial design, participants typically chose the strategy of prioritizing one task over the other, with poor performance in the non-prioritized task. Thus, the blocked design with explicit task instructions ensured equal performance and physically identical stimuli in the two tasks (both targets were shown on each trial, but only one was task relevant in each block). Psychophysical performance was matched between integration and segregation tasks by selecting a critical ISI for each participant (see the Psychophysics section in Results). In experiment 1, the two displays (10-ms duration each + subject-specific ISI) were presented after a randomly jittered pre-stimulus time period (1–2 s) and followed by a response screen after 500 ms. MEG was recorded continuously to contrast pre-stimulus oscillatory activity, the stimulus-evoked fields, frequency-specific phase coherence, and MVPA decoding between tasks. In experiment 2, we timed stimulus presentation (10 ms for each display + 50-ms ISI) relative to eye fixation onset and contrasted the fixation-aligned behavioral time courses (500 ms in Expt 2A, and 1,000 ms in Expt 2B) between tasks. A complete description of the materials and methods can be found in the online Supplemental Experimental Procedures.

SUPPLEMENTAL INFORMATION

Supplemental Information includes six figures, six tables, and Supplemental Experimental Procedures and can be found with this article online at http://dx.doi.org/10.1016/j.cub.2016.04.070.

AUTHOR CONTRIBUTIONS

Conceptualization, A.W. and D.M.; Methodology, A.W.; Formal Analysis, A.W.; Investigation, A.W. and E.M.; Writing – Original Draft, A.W. and D.M.; Writing – Review & Editing, A.W., N.W., and D.M.; Visualization, A.W.; Funding Acquisition, D.M.; Resources, M.G.v.K. and N.W.; Supervision, D.M.

ACKNOWLEDGMENTS

REFERENCES

1. Hecht, S., and Smith, E.L. (1936). Intermittent stimulation by light VI. Area and the relation between critical frequency and intensity. J. Gen. Physiol. 19, 979–989.

2. Sweet, A.L. (1953). Temporal discrimination by the human eye. Am. J. Psychol. 66, 185–198.

3. Westheimer, G., and McKee, S.P. (1977). Perception of temporal order in adjacent visual stimuli. Vision Res. 17, 887–892.

4. Burr, D.C., and Ross, J. (1982). Contrast sensitivity at high velocities. Vision Res. 22, 479–484.

5. Lee, B.B., Pokorny, J., Smith, V.C., Martin, P.R., and Valberg, A. (1990). Luminance and chromatic modulation sensitivity of macaque ganglion cells and human observers. J. Opt. Soc. Am. A 7, 2223–2236.

6. Spekreijse, H., van Norren, D., and van den Berg, T.J.T.P. (1971). Flicker responses in monkey lateral geniculate nucleus and human perception of flicker. Proc. Natl. Acad. Sci. USA 68, 2802–2805.

7. Martinez-Conde, S., Macknik, S.L., and Hubel, D.H. (2002). The function of bursts of spikes during visual fixation in the awake primate lateral geniculate nucleus and primary visual cortex. Proc. Natl. Acad. Sci. USA 99, 13920–13925.

8. Burr, D. (1980). Motion smear. Nature 284, 164–165.

9. Oğmen, H., and Herzog, M.H. (2010). The geometry of visual perception: Retinotopic and nonretinotopic representations in the human visual system. Proc. IEEE Inst. Electr. Electron Eng. 98, 479–492.

10. Wutz, A., and Melcher, D. (2014). The temporal window of individuation limits visual capacity. Front. Psychol. 5, 952.

11. Wutz, A., and Melcher, D. (2013). Temporal buffering and visual capacity: the time course of object formation underlies capacity limits in visual cognition. Atten. Percept. Psychophys. 75, 921–933.

12. Zimmermann, E., Morrone, M.C., and Burr, D.C. (2013). Spatial position information accumulates steadily over time. J. Neurosci. 33, 18396–18401.

13. Rüter, J., Marcille, N., Sprekeler, H., Gerstner, W., and Herzog, M.H. (2012). Paradoxical evidence integration in rapid decision processes. PLoS Comput. Biol. 8, e1002382.

14. Di Lollo, V. (1977). Temporal characteristics of iconic memory. Nature 267, 241–243.

15. Buzsáki, G. (2006). Rhythms of the Brain (Oxford University Press).

16. Samaha, J., and Postle, B.R. (2015). The speed of alpha-band oscillations predicts the temporal resolution of visual perception. Curr. Biol. 25, 2985–2990.

17. Breitmeyer, B.G., and Öğmen, H. (2006). Visual Masking: Time Slices through Conscious and Unconscious Vision (Oxford University Press).

18. Fracasso, A., Caramazza, A., and Melcher, D. (2010). Continuous perception of motion and shape across saccadic eye movements. J. Vis. 10, 14.

19. Eriksen, C.W., and Collins, J.F. (1967). Some temporal characteristics of visual pattern perception. J. Exp. Psychol. 74, 476–484.

20. Hogben, J.H., and di Lollo, V. (1974). Perceptual integration and perceptual segregation of brief visual stimuli. Vision Res. 14, 1059–1069.

21. Cousineau, D. (2005). Confidence intervals in within-subject designs: a simpler solution to Loftus's and Masson's method. Tutor. Quant. Methods Psychol. 1, 42–45.

22. Wutz, A., Weisz, N., Braun, C., and Melcher, D. (2014). Temporal windows in visual processing: "prestimulus brain state" and "poststimulus phase reset" segregate visual transients on different temporal scales. J. Neurosci. 34, 1554–1565.

23. Thut, G., Miniussi, C., and Gross, J. (2012). The functional importance of rhythmic activity in the brain. Curr. Biol. 22, R658–R663.

24. Makeig, S., Westerfield, M., Jung, T.P., Enghoff, S., Townsend, J., Courchesne, E., and Sejnowski, T.J. (2002). Dynamic brain sources of visual evoked responses. Science 295, 690–694.

25. Busch, N.A., Dubois, J., and VanRullen, R. (2009). The phase of ongoing EEG oscillations predicts visual perception. J. Neurosci. 29, 7869–7876.

26. Landau, A.N., and Fries, P. (2012). Attention samples stimuli rhythmically. Curr. Biol. 22, 1000–1004.

27. Song, K., Meng, M., Chen, L., Zhou, K., and Luo, H. (2014). Behavioral oscillations in attention: rhythmic α pulses mediated through θ band. J. Neurosci. 34, 4837–4844.

28. Fiebelkorn, I.C., Saalmann, Y.B., and Kastner, S. (2013). Rhythmic sampling within and between objects despite sustained attention at a cued location. Curr. Biol. 23, 2553–2558.

29. Huang, Y., Chen, L., and Luo, H. (2015). Behavioral oscillation in priming: competing perceptual predictions conveyed in alternating theta-band rhythms. J. Neurosci. 35, 2830–2837.

30. Melcher, D., and Colby, C.L. (2008). Trans-saccadic perception. Trends Cogn. Sci. 12, 466–473.

31. Schroeder, C.E., Wilson, D.A., Radman, T., Scharfman, H., and Lakatos, P. (2010). Dynamics of Active Sensing and perceptual selection. Curr. Opin. Neurobiol. 20, 172–176.

32. Ito, J., Maldonado, P., Singer, W., and Grün, S. (2011). Saccade-related modulations of neuronal excitability support synchrony of visually elicited spikes. Cereb. Cortex 21, 2482–2497.

33. Bartlett, A.M., Ovaysikia, S., Logothetis, N.K., and Hoffman, K.L. (2011). Saccades during object viewing modulate oscillatory phase in the superior temporal sulcus. J. Neurosci. 31, 18423–18432.

34. Jutras, M.J., Fries, P., and Buffalo, E.A. (2013). Oscillatory activity in the monkey hippocampus during visual exploration and memory formation. Proc. Natl. Acad. Sci. USA 110, 13144–13149.

35. Ringo, J.L., Sobotka, S., Diltz, M.D., and Bunce, C.M. (1994). Eye movements modulate activity in hippocampal, parahippocampal, and infero-temporal neurons. J. Neurophysiol. 71, 1285–1288.

36. Hoffman, K.L., Dragan, M.C., Leonard, T.K., Micheli, C., Montefusco-Siegmund, R., and Valiante, T.A. (2014). Saccades during visual explora-tion align hippocampal 3–8 Hz rhythms in human and non-human primates. Front. Syst. Neurosci. 7, 43.

37. Panzeri, S., Ince, R.A., Diamond, M.E., and Kayser, C. (2014). Reading spike timing without a clock: intrinsic decoding of spike trains. Philos. Trans. R. Soc. Lond. B Biol. Sci. 369, 20120467.

38. Akyürek, E.G., Schubö, A., and Hommel, B. (2010). Fast temporal event integration in the visual domain demonstrated by event-related potentials. Psychophysiology 47, 512–522.

39. Kok, P., Jehee, J.F., and de Lange, F.P. (2012). Less is more: expectation sharpens representations in the primary visual cortex. Neuron 75, 265–270.

40. Thorpe, S., Delorme, A., and Van Rullen, R. (2001). Spike-based strategies for rapid processing. Neural Netw. 14, 715–725.

41. Ross, J., Morrone, M.C., Goldberg, M.E., and Burr, D.C. (2001). Changes in visual perception at the time of saccades. Trends Neurosci. 24, 113–121.

42. Neri, P., Morrone, M.C., and Burr, D.C. (1998). Seeing biological motion. Nature 395, 894–896.

43. Bishop, G. (1933). Cyclical changes in excitability of the optic pathway of the rabbit. Am. J. Physiol. 103, 213–224.

44. Varela, F.J., Toro, A., John, E.R., and Schwartz, E.L. (1981). Perceptual framing and cortical alpha rhythm. Neuropsychologia 19, 675–686.

45. Cecere, R., Rees, G., and Romei, V. (2015). Individual differences in alpha frequency drive crossmodal illusory perception. Curr. Biol. 25, 231–235.

46. VanRullen, R., and Koch, C. (2003). Is perception discrete or continuous? Trends Cogn. Sci. 7, 207–213.

47. Scharnowski, F., Rüter, J., Jolij, J., Hermens, F., Kammer, T., and Herzog, M.H. (2009). Long-lasting modulation of feature integration by transcranial magnetic stimulation. J. Vis. 9, 1–10.

48. VanRullen, R., and Macdonald, J.S. (2012). Perceptual echoes at 10 Hz in the human brain. Curr. Biol. 22, 995–999.

49. Drewes, J., Zhu, W., Wutz, A., and Melcher, D. (2015). Dense sampling reveals behavioral oscillations in rapid visual categorization. Sci. Rep. 5, 16290.